Published in final edited form as:
J Comp Neurol. 2008 October 1; 510(4): 440–461. doi:10.1002/cne.21805.

Thalamic connections of architectonic subdivisions of temporal cortex in grey squirrels (*Sciurus carolinenesis*)

Peiyan Wong[1], **Omar A. Gharbawie**[1], **Lynn E. Luethke**[1,2], and **Jon H. Kaas**[1,*]

[1] Department of Psychology, Vanderbilt University, Nashville TN 37212

[2] Now at Center for Scientific Review, National Institutes of Health, Bethesda MD 20892

Abstract

The temporal cortex of grey squirrels contains three architectonically distinct regions. One of these regions, the temporal anterior (Ta) region has been identified in previous physiological and anatomical studies as containing several areas that are largely auditory in function. Consistent with this evidence, Ta has architectonic features that are internally somewhat variable, but overall sensory in nature. In contrast, the caudally adjoining temporal intermediate region (Ti) has architectonic features that suggest higher order and possibly multisensory processing. Finally, the most caudal region, composed of previously defined temporal medial (Tm) and temporal posterior (Tp) fields, again has more of the appearance of sensory cortex. To better understand their functional roles, we injected anatomical tracers into these regions to reveal their thalamic connections. As expected, the dorsal portion of Ta, containing two primary or primary-like auditory areas, received inputs from the ventral and magnocellular divisions of the auditory medial geniculate complex, MGv and MGm. The most caudal region, Tm plus Tp, received inputs from the large visual pulvinar of squirrels, possibly accounting for the sensory architectonic characteristics of this region. However, Tp additionally receives inputs from the magnocellular (MGm) and dorsal (MGd) divisions of the medial geniculate complex, implicating Tp in bisensory processing. Finally, the middle region, Ti, had auditory inputs from MGd and MGm, but not from the visual pulvinar, providing evidence that Ti has higher-order auditory functions. The results indicate that the architectonically distinct regions of temporal cortex of squirrels are also functionally distinct. Understanding how temporal cortex is functionally organized in squirrels can guide interpretations of temporal cortex organization in other rodents where architectonic subdivisions are not as obvious.

Keywords

visual cortex; auditory cortex; multisensory cortex; lateral geniculate nucleus; pulvinar; rodents; medial geniculate; supragenicular

Introduction

Temporal cortex lies in a posteroventral portion of the neocortex, and it is heavily involved in auditory and visual processing in most mammals. In squirrels, three distinct divisions of temporal cortex were previously described by Kaas et al. (1972). The most anterior division, the temporal anterior area (Ta) has features of sensory cortex in Nissl and myelin stained

*Correspondence to: Jon H. Kaas, Vanderbilt University, 301 Wilson Hall, 111 21st Avenue South, Nashville, TN 37203, Phone: 615-322-6029, Fax: 615-343-8449, E-mail: jon.kaas@vanderbilt.edu.
Associate Editor: Joseph Price

sections. Thus, layer 4 is broad, well defined, and packed with cells. Also, the inner and outer bands of Baillarger are densely myelinated. Ta was subsequently shown to contain two auditory areas: a primary area, A1, and a primary-like rostral area, R (Merzenich et al., 1976; Luethke et al., 1988), as well as remaining, more ventral, auditory areas. In contrast, immediately posterior to Ta, the temporal intermediate area (Ti) has a poorly developed layer 4, and layer 5 has a more superficial sublayer packed with cells and a deeper sublayer of more scattered, larger cells. In addition, Ti is poorly myelinated. Thus, Ti does not have the architectonic features that distinguish primary and sometimes secondary areas of sensory cortex. Finally, the most posterior division of temporal cortex, the temporal posterior area (Tp) has a distinct layer 4 that is less prominent than in Ta, but more than in Ti. However, the outer and inner bands of Baillarger are distinct in myelin stains. Overall, Tp appears to have some of the architectonic features of sensory cortex, although they are not as pronounced as in Ta.

A more recent architectonic investigation (Wong and Kaas, 2008) based on an array of immunohistochemical and histochemical procedures identified and further characterized the same three divisions of temporal cortex. In addition, Wong and Kaas (2008) provided evidence for an additional temporal cortex division, the temporal mediodorsal field (Tm) medial to Tp. Most or all of Ta is involved in auditory processing, while Ti, Tp and Tm are in regions of temporal cortex that are expected to be involved in auditory, visual, or multisensory processing. Here, the functional roles of these divisions of temporal cortex are explored by determining their connections with thalamic nuclei. Such investigations of thalamocortical connections of temporal cortex in squirrels have been limited. However, lesions that included Ti and Tp resulted in retrograde degeneration of neurons in the visual pulvinar, and a lesion involving Ta and adjoining cortex resulted in cell loss in the medial geniculate complex and the visual pulvinar (Kaas et al., 1972). Furthermore, a lesion in the posterior part of the pulvinar produced anterograde degeneration of axon terminals in Tp and the region we now define as Tm, and an injection of a tracer at the Ti/Tp border labeled neurons in the posterior pulvinar (Robson and Hall, 1977). These limited results suggest that divisions of temporal cortex in squirrels are involved in auditory, visual or auditory-visual processing.

The objective of the present study was to explore the thalamocortical connections of the four temporal cortex subdivisions in squirrels more extensively using modern anatomical tracing procedures, as well as immunohistochemical procedures to identify thalamic nuclei. Here, we describe the distributions of retrogradely labeled neurons in the medial geniculate complex and the visual pulvinar after injections of tracers in Ta, Ti, Tp and Tm. We also briefly illustrate the architecture of temporal cortex, and the auditory and visual thalamus. The results implicate Ta in auditory processing, Tm in visual processing, Tp in predominantly visual but also auditory processing, and Ti in higher-order auditory processing.

Materials and Methods

Animals

Twelve grey squirrels (*Sciurus carolinensis)* weighing between 300–400 g were studied, and tracer injections were made in ten of them (Table 2). The experiments were conducted in compliance with the guidelines of Vanderbilt University Animal Care and Use Committee and followed National Institute of Health guidelines. Squirrels were individually housed in wire mesh cages in a colony room maintained on a 12/12 h light/dark cycle (06:00–18:00 h).

Tracers

The neuroanatomical tracers used in the present study included: wheat germ agglutinin-horseradish peroxidase (WGA-HRP, Sigma, St. Louis, MO, 2% in distilled water); cholera toxin b-subunit (CTB, Molecular Probes Invitrogen, Carlsbad, CA, 10% in distilled water); Fluoro Ruby (FR, Molecular Probes Invitrogen, Carlsbad, CA, 10% in distilled water); Fast Blue (FB, Polysciences Inc., Warrington, PA, 3% in distilled water); diamidino yellow (DY, Sigma, St. Louis, MO, 2% in distilled water); Fluoro-Gold (FG, Molecular Probes Invitrogen, Carlsbad, CA, 10% in distilled water). A total volume of 0.05 μl was injected for WGA-HRP; 0.1–0.3 μl was injected for FG, FB and DY; 0.3–0.6 μl was injected for FR and CTB. Injections locations are summarized in Table 2.

Surgery

Surgeries were conducted under aseptic conditions in anesthetized animals. Squirrels were initially anesthetized with ketamine hydrochloride (70 mg/kg, i.p.). Lidocaine hydrochloride was locally injected into the ears before securing the skull in the stereotaxic apparatus and under the scalp before making an incision. During surgery, inhalation anesthesia was delivered through a mask and isoflurane flow was adjusted to 2%. The head was tilted laterally to facilitate access to temporal cortex. A small portion of the temporal muscle was dissected from the parietal bone and retracted. The skull overlaying auditory cortex was trephinated, and the dura was cut and deflected. The exposed cortex was digitally photographed to guide microelectrode penetrations and/or tracer injections.

Multiunit microelectrode recording

In a previous study (Leuthke et al., 1988), cortical areas A1 and R were electrophysiologically defined, and tracers were injected into A1 and R, and adjoining auditory cortex. The physiological results, as well as the cortical connections revealed in this study can be found in this earlier publication. Here, we describe the previously unpublished thalamic connections from these cases, as well as the results from additional cases with injections caudal to auditory cortex. In these earlier experiments, multiunit microelectrode mapping was conducted to identify the locations and extents of primary auditory cortex (A1) and the rostral auditory area (R) within the anterior auditory region for subsequent tracer injections in A1 and R (see Leuthke et al., 1988 for details). The exposed cortex was covered with an inert silicon fluid. Recordings were made with low impedance tungsten microelectrodes (0.9–1.2 M at 1,000 Hz). A hydraulic microdrive was used to lower the tip of the electrode between 900–1200 mm beneath the surface of the neocortex, which is the approximate location of layer IV cell bodies that receive thalamic afferents. Depths responsive to auditory stimuli were noted.

At each recording site, auditory stimuli were presented to the contralateral ear via hollow ear tubes coupled to audiometric drivers were calibrated prior to each experiment by using a one-half-inch condenser microphone coupled to a one-third octave band filter and sound level meter. Pure tone stimuli were generated and the sound pressure level of the stimuli was regulated by a Krohn-Hite oscillator and shaped by an electronic switch with rise-fall time of 6 msec and duration of 100 msec. Stimuli were presented at the approximate rate of one per second.

Neuronal responses were amplified, filtered, and displayed. Best frequencies in given penetrations were determined by varying stimulus frequency and intensity until a threshold response was obtained. Patterns of tonotopic organization were determined by obtaining the best frequencies for a number of closely spaced recording sites. In some penetrations, neural clusters were responsive to auditory clicks (produced by tapping two metal rods together) but not to pure tones. Somatosensory receptive fields were obtained by lightly touching the

skin and moving hairs on the body surface with fine probes. Borders of auditory fields A1 and R were defined by a reversal in tonotopic organization noted across rows of recording sites, and other borders were revealed by a marked change in responsiveness to tonal or other auditory stimuli.

Tracer injections

At the completion of the microelectrode mapping of auditory cortex, WGA-HRP was pressure injected into A1 or R. Results from five cases are shown here. The tracer was delivered from a Hamilton syringe fitted with a glass pipette beveled to a fine tip. In addition, several tracers were injected in areas Ti, Tm, and Tp in five other squirrels. Injection locations for these cases were primarily guided by blood vessel patterns of the exposed cortex, as well as results from the cases that involved microelectrode mapping. One to three tracers (see Table 1) were injected in different locations in each case. Injections were made at 400 and 800 μm depths from the surface of the cortex, and the needle tip was left at each site for 5 min to allow tracer diffusion. Any leakage of tracer during the injections was removed with a cotton swab or sterile saline flushes to prevent artifactual spread. The cortex was then covered with gelatin film, and the skull opening was sealed with an artificial bone flap made of dental cement. The scalp was sutured, and treated with a topical antibiotic ointment. Animals were carefully monitored during recovery from anesthesia until fully awake, at which time they were received Bupernex (0.3 mg/kg, i.m.) for the relief of any possible pain or discomfort. Each animal was then returned to its home cage with soft food and water available *ad libitum*.

Histology

Three to six days after surgery, animals were injected with a lethal dose of sodium pentobarbital (80mg/kg), and when areflexional, perfused with phosphate-buffered saline (PBS; pH 7.4), followed by 2% paraformaldehyde in PBS and 2% paraformaldehyde in PBS with 10% sucrose solution. The brain was removed and the cortex was separated from the brainstem. The right and left hemispheres of the cortex were separated, and flattened between two glass slides. The flattened cortices and brain stem were submerged in a 30% sucrose solution for cryoprotection overnight.

The flattened cortex and brainstem were respectively sectioned in the tangential and coronal planes at 40 μm thickness on a freezing microtome. Cortical and brainstem sections were saved in series that depended on the tracers injected and immunohistochemical staining planned. In cases with fluorescent tracer injections (conjugated CTB, DY, FR, or FG), one series of sections was mounted onto glass slides without further processing for fluorescence microscopy. In one case, a series was processed with a DAB reaction to reveal the CTB tracer injection for light microscopy. In cases with WGA-HRP injections, a series was processed for tetramethylbenzidine (TMB) (Mesulam, 1978).

To reveal architectonic features of the flattened cortex, additional series were processed for cytochrome oxidase (CO; Wong-Riley, 1979) and myelin (Gallyas, 1979). Architectonic features of thalamic nuclei from the same cases were also visualized using CO, and myelin and Nissl stains. The brainstem was harvested from two additional squirrels that did not receive tracer injections for additional architectonic analysis. Series from those two cases were immuhistochemically stained for (see Table 2): SMI-32 (mouse monoclonal anti-SMI-32 from Covance Inc. Princeton, NJ; 1:2000), parvalbumin (PV) (mouse monoclonal anti-PV from Sigma-Aldrich, St. Louis, Mo; 1:2000), calbindin (CB) (mouse monoclonal anti-CB from Swant, Bellinzona, Switzerland; 1:5000), vesicle glutamate transporter 2 (VGluT2) (mouse monoclonal anti-VGluT2 from Chemicon now part of Millipore,

Billerica, MA; 1:2000). Sections were reacted using the protocol described in Ichinohe et al. (2003).

The mouse monoclonal anti-SMI-32 antibody specifically recognized the 200-kD nonphosphorylated epitope in neurofilament H of most mammalian species (manufacturer's technical information) and reveals a subset of pyramidal cells (Campbell and Morrison, 1989). PV is a calcium-binding protein present in subsets of GABAergic, non-pyramidal cells, thought to be basket and double bouquet interneurons (Celio, 1986; Condé et al., 1996; DeFelipe, 1997; Hof et al., 1999). The mouse monoclonal anti-parvalbumin antibody specifically recognizes the Ca-binding spot of parvalbumin (MW= 12,000) from human, bovine, goat, pig, canine, feline, rabbit, rat, frog, and fish on a two-dimensional gel (manufacturer's technical information). CB is another calcium-binding protein that reveals a different subset of GABA immunoreactive interneurons from PV (Van Brederode et al., 1990), and the mouse monoclonal anti-calbindin antibody specifically stains the 45Ca-binding spot of calbindin D-28K (MW 28,000, IEP 4.8) from human, monkey, rabbit, rat, mouse and chicken in a two-dimensional gel (manufacturer's technical information). VGluT2 immunostaining reveals the thalamocortical terminations in layer 4 (Fujiyama et al., 2001; Kaneko and Fujiyama, 2002; Nahami and Ersir, 2005), has a predicted molecular weight of 60kDa in western blots (as shown by a comparable product from Abcam Inc. Cambridge, MA), and reacts specifically with the rat and mouse (manufacturer's technical information). The SMI-32, PV, CB, and VGluT2 immunostaining patterns in the squirrel is consistent with findings reported in other rodents, such as rats (Van De Werd and Uylings, 2008, Ichinohe et al., 2003).

Data analysis

Distributions of neurons labeled with FR, FG, DY, and CTB in the brainstem were plotted with a fluorescent microscope using Igor Pro (WaveMetrics, Inc.). The brainstem sections processed for TMB were drawn at low magnification by using a drawing tube attached to a lightfield/darkfield microscope and the regions of WGA-HRP label were located under darkfield illumination. Processed sections were also viewed under a Nikon E800 microscope and digital images were acquired using a Microlumina Leaf digital camera mounted on the microscope. The digitized images were adjusted for brightness and contrast using Adobe Photoshop, but they were not otherwise altered.

Architectonics

Series of sections were stained to reveal cytoarchitecture to confirm tracer injection locations and to identify the locations of retrograde label in the thalamic nuclei. Stained sections were viewed under a Nikon E800 microscope (Nikon Inc., Melville, NY) and digital photomicrographs of sections were acquired using a Nikon DXM1200 camera (Nikon Inc., Melville, NY) mounted on the microscope. Digitized images were adjusted for levels, brightness and contrast using Adobe Photoshop (Adobe Systems Inc., San Jose, CA), but they were not otherwise altered. Cortical borders were primarily identified from myelin stained sections. In ten cases involving tracer injections, subdivisions of thalamic nuclei were delineated from Nissl, CO, and myelin stained sections. Drawings of areal and nuclear boundaries in cortical and thalamic sections stained for architectonics were aligned with tracer plots of labeled cells using common blood vessels and landmarks. The architectonics of thalamic subdivisions were studied further in the two cases that did not receive tracer injections, as their brainstems were studied after immunohistochemical staining for architectonic borders.

Results

The present study describes the pattern of thalamocortical projections from areas Ta, Ti, Tp, and Tm of the temporal cortex in grey squirrels. The major thalamic nuclei that project to these temporal areas include the pulvinar and nuclei of the medial geniculate complex (MGC), the dorsal, MGd, ventral, MGv, magnocellular, MGm and suprageniculate, SG, nuclei. The pulvinar and part of the MGC can be seen on the ventrolateral surface of the diencephalon when the overlying cortex is removed (Fig. 1). We first present architectonic characteristics of each of the four temporal areas that allowed us to determine the location of our injections, followed by the architectonic characteristics of the relevant thalamic nuclei and last, the patterns of thalamic projections that were labeled by the temporal cortex injections.

Architectonic characteristics of the subdivisions of the temporal cortex

The temporal cortex of grey squirrels occupies a relatively large region and consists of three architectonically distinct subdivisions. They include the anterior temporal field, Ta, which contains the primary auditory area (A1) and the rostral area (R); the intermediate temporal area, Ti; and the posterior temporal area, Tp. The mediodorsal temporal field, Tm, architectonically resembles Tp, but several differences have been observed. The boundaries of these four temporal subdivisions can be most reliably identified in stained brain sections cut in the coronal or the horizontal planes (see Wong and Kaas, 2008). However, the full extents of the areas arebetter appreciated in brains where cortex has been separated from the underlying white matter, flattened, and cut parallel to the cortical surface. The cortical sections were processed for myelin (Fig. 2D). These subdivisions are briefly described here. For a more extensive description, see Wong and Kaas (2008).

Ta, the most anterior of the temporal subdivisions, is identified as a densely myelinated oval (Fig. 2C and D) surrounded by less well-myelinated areas such as the parietal ventral area rostrally and the parietal lateral (Pl) area dorsally. Areas caudal and ventral to Ta include Ti and perirhinal areas respectively, which are very poorly myelinated. However, the density of myelination within Ta is not homogenous, suggesting the presence of additional subdivisions. The dorsal half of Ta, containing two primary auditory areas (A1 and the rostral area, R), is more densely myelinated than the rest of Ta. In addition, A1 is slightly more densely myelinated than the other primary auditory area, R. In Nissl preparations, Ta has a well-developed layer 4, which is densely packed with darkly stained neurons (Fig. 1B).

The most caudal region of the temporal cortex consists of two areas, Tp and Tm. Both areas Tp and Tm are well myelinated, with Tp having a slightly higher density of myelination than Tm. Area Tm was previously included as a peripheral part of area 19, 19p, or part of Tp, but our recent architectonic characterizations, using multiple immunohistological stains, distinguished Tm as a separate subdivision of the temporal cortex (Wong and Kaas, 2008). In Nissl preparations, layer 4 of Tm is slightly more densely packed with cells than layer 4 of area 19 proper. Tm is also somewhat more densely myelinated than area 19.

Ti is a large, poorly myelinated field between Ta and Tp. This architectonic feature allows the easy identification of the rostral border of Ti with Ta, caudal border with Tp and dorsal border with Pl and Tm. Also, the cells in layer 4 of Ti area not as densely packed and darkly stained in Nissl preparations as those in Tp and Ta, and cells in layer 5 are more darkly stained, so that overall, layers are less distinct in Ti.

Architectonic characteristics of the thalamic nuclei

In this study, we used a number of histological stains, such as those for Nissl substance, myelin, CO and, ACHE, and immunohistochemical stains, such as those for VGluT2, CB,

PV, and SMI-32, in sets of serial sections to reveal the thalamic nuclei, and characterize them in greater detail. Coronal sections of the thalamus from these preparations are shown in Figure 3. The sections are from three levels in an anterior to posterior progression. Figures 3A–L, M–U and V–X are photomicrographs of sections taken from three different brains.

The pulvinar complex—At the anterior level, the pulvinar lies medial to the dorsal lateral geniculate nucleus (dLGN). More posteriorly, the pulvinar shifts laterally and ventrally as the dLGN reduces in size, and extends further posteriorly than the dLGN. Robson and Hall (1977) described three subdivisions of the pulvinar complex from Nissl-stained sections. For purposes of the present paper, it is not critical for us to distinguish between the subdivisions of the pulvinar, and the architectonic characteristics of the pulvinar complex are described as a whole.

The pulvinar is separated from dLGN by a band of white matter that is prominent in most of the stains, such as the Nissl stain. There is a lowered packing density of cells in the pulvinar, compared to dLGN (Fig. 3A). Anteriorly, in Nissl-stained sections, the lateral portion of the pulvinar is more densely populated with cells than the medial portion (Fig. 3A). More posteriorly, the cells in the lateral portion of the pulvinar stain less darkly for Nissl substance compared to the cells in the medial portion (Fig. 3B). In the most posterior sections, the pulvinar is occupied by larger, more darkly stained cell bodies than in the anterior sections, with no obvious difference between the lateral and medial portions of the pulvinar (Fig. 3C). The anterior part pulvinar is more lightly myelinated than dLGN, especially in the lateral portion, with some horizontal fibers running through the medial portion (Fig. 3D, 3E). Posteriorly, the pulvinar is densely myelinated (Fig. 3F). CO expression in the pulvinar is rather homogenous in the more anterior sections, and is lower than in the dLGN (Fig. 3G). More posteriorly, the medial region of the pulvinar has higher expression of CO than the lateral region (Fig. 3H), whereas most posteriorly, the reverse is observed (Fig. 3I).

In sections immunostained for VGluT2, the pulvinar is as darkly stained as dLGN in anterior sections, with the dorsomedial portion expressing more intense staining than the rest of the pulvinar (Fig. 3J). Posteriorly, the pulvinar shows more intense staining for VGluT2 than the anterior part of the pulvinar (Figs. 3K, 3L). The level of CB-expression in the pulvinar is slightly higher than in dLGN, with medial portion of the pulvinar being more intensely stained and containing some darkly stained CB-immunopositive cells (Fig. 3M). CB expression in the pulvinar is almost absent in the most posterior sections (Figs. 3N, 3O). PV-immunoreactivity is mostly absent in the pulvinar (Figs. 3P to 3R). The pulvinar is strongly reactive for the SMI-32 antibody and for AChE through its anterior to posterior length, with no visible difference between the medial and lateral portions (Figs. 3S to 3X).

The medial geniculate complex—The medial geniculate complex (MGC) is located in the posterior region of the thalamus and consists of at least three subdivisions, MGd, MGv, and MGm. We also describe the SG as a nucleus with auditory and other functions. The anterior portion of the MGC is ventral and medial to the dLGN and pulvinar and dorsal to the ventroposterior complex. Posteriorly, the ventral subdivision of the MGC protrudes laterally, forming a distinct bump on the ventrolateral surface of the diencephalon (Fig. 1).

Medial geniculate ventral (MGv) subdivision: In grey squirrels, MGv occupies about 55% of the total volume of the MGC (Krubitzer and Kaas, 1987) and stands out as an oval-shaped nucleus that is densely packed with small and medium-sized cells (Figs. 3A to 3C). MGv is more intensely stained, for CO (Figs. 3G, 3H) and ACHE (Fig. 3V, 3W) compared to the surrounding medial geniculate subdivisions. CO and ACHE staining in MGv is more intense in anterior sections (Fig. 3G, 3H, 3V, 3W), than in the most posterior sections (Figs. 3I, 3X).

MGv is more myelinated than MGd, but less myelinated than MGm (Figs. 3D to F). Within MGv, the anteriomedial portion is more heavily myelinated than the posterior portion.

MGv is more intensely immunoreactive for VGluT2 than most of the surrounding medial geniculate nuclei, except for MGm (Fig. 3J to 3L). VGluT2 staining is not homogenous in the anterior sections (Fig. 3J, 3K), whereas staining is more even in posterior sections (Fig. 3L). MGv is very lightly stained for CB in the anterior sections compared to MGd and SG, but is more darkly stained than MGm (Figs. 3M, 3N). In the posterior sections, MGv shows slightly increased CB staining (Fig. 3O). In contrast, the posterior portion of MGv has almost no PV (Fig. 3R) nor SMI-32 (Fig. 3U) staining. Anteriorly, MGv is more darkly stained for PV (Figs. 3P, 3Q) and SMI-32 (Figs. 3S, 3T) than MGd and SG, but the staining intensities are less than that of MGm.

Medial geniculate dorsal (MGd) subdivision: MGd lies between the pulvinar and MGv throughout the anterior-posterior length of the MGC. MGd is the second largest subdivision in the MGC, and occupies about 30% of the MGC (Krubitzer and Kaas, 1987). Anteriorly, MGd is large and somewhat pyramidal-shaped, and shrinks in size posteriorly. In Nissl stained sections, MGd is easily differentiated from MGv because it is less densely populated with cells and the cells are larger than those in MGv (Figs. 3A to 3C). MGd is less myelinated than both MGv and MGm (Figs. 3D to 3F). The CO staining in MGd is more intense than in MGm, but less than in MGv and SG (Figs. 3G to 3I). ACHE expression is weak in MGd (Figs. 3V to 3X).

In VGluT2 immunostained sections, MGd is more lightly stained than MGm and only slightly less stained than MGv (Figs. 3J, 3K) in anterior sections, but no perceptible difference between the three nuclei is observed in the posterior most section (Fig. 3L). Anteriorly, in sections stained for CB, MGd is more darkly stained than MGv and MGm, but is less darkly stained than SG (Figs. 3M, 3N). Posteriorly, some CB-immunopositive cells are observed in MGd, but MGd is less darkly stained than MGv at this level (Fig. 3L). The converse is observed in PV preparations. MGd is very poorly stained compared to MGv and MGm, but is more darkly stained than SG in anterior sections (Figs. 3P, 3Q). In the posterior most section, MGd is more darkly stained than MGv (Fig. 3R). The anterior potion of MGd is very lightly stained in SMI-32 preparations, and the staining is only slightly more intense than in SG (Fig. 3S).

Medial geniculate magnocellular (MGm) subdivision: Anteriorly, MGm lies ventral to MGv. In a posterior progression, MGm moves dorsally to lie more medially between MGv and MGd. Mgm is the third smallest subdivision in the MGC, and occupies about 15 to 20% of the MGC (Krubitzer and Kaas, 1987). In Nissl-stained sections, MGm is sparsely populated with a mixture of large, medium and small cells (Figs. 3A to 3C). MGm is the most densely myelinated of the MGC subdivisions (Figs. 3D to 3F). The expression levels of CO (Fig. 3G, 3H) and ACHE (Fig. 3V, 3X) is lower in MGm, in comparison with the rest of the MGC subdivisions, although the differences in staining intensities are not obvious in the posterior extent of the MGC (Fig. 3I, 3X).

The anterior portion of MGm stains more darkly for VGluT2 than the other MGC subdivisions (Fig. 3J, 3K), and the contrast is especially distinct at the dorsal border with SG (Fig. 3K). Throughout its anterior-posterior length, MGm is poorly stained in CB preparations (Figs. 3M to 3O). Similar to MGv, MGm stains intensely in PV sections (Figs. 3P to 3R), but unlike MGv, the posterior portion of MGm is also darkly stained for PV (Fig. 3R). In SMI-32 preparations, MGm is the most intensely stained of all the MGC subdivisions (Figs. 3S to 3U).

Suprageniculate (SG) subdivision: SG is a small nucleus that lies medial to MGd and dorsal to MGm. In the middle section, which is the approximate midpoint through the anterior-posterior length of the MGC, SG appears to be distinct from MGd. At that level, the dLGN is almost absent, and the superior colliculus (SC) is rather large. SG is no longer distinct at the level where MGv protrudes from the diencephalon and the SC is very large. The cells in SG are larger than those in MGd (Figs. 3b, 3C), and SG is the least myelinated of all the MGC subdivisions, with some sparse horizontal fiber bundles running through (Figs. 3D, 3E). SG stains moderately for CO (Fig. 3H) and very darkly for ACHE (Figs. 3V 3W).

SG is readily differentiated from the subdivisions of MGC because of its low or nearly absent immunoreactivity for the VGLuT2 (Fig. 3K), PV (Fig. 3Q) and SMI-32 (Fig. 3T) antibodies. In CB preparations, SG is darkly stained, with the presence of CB-immunopositive neurons (Fig. 3Q).

Thalamocortical connections

Thalamocortical connections of A1—Injections of WGA-HRP were placed in A1 of three grey squirrels. In case 15 (Fig. 4), the injection core was completely confined to A1 and dense foci of retrogradely labeled neurons and terminals were concentrated in MGv. In the posterior thalamic sections, a few labeled cells were present in MGm. When the injection core was largely within A1, with significant spread into Ti (case 21, Fig. 5), the majority of labeled cells were in MGv, with many labeled cells in anterior MGd and posterior MGm. In case 41, a dense patch of labeled cells and terminals was observed in MGv, when the injection site was mostly confined to A1, with a marginal spread into cortex ventral to A1, the anterior temporal intermediate area (Ta_i) (Fig. 6). However, some labeled cells were present in anterior MGd and posterior MGm as well.

From the results, we can conclude that MGv provides the major source of thalamocortical projections to A1, while some minor projections to A1 originate from the posterior part of MGm. In cases where the injection site involved cortex posterior or ventral to A1, labeled cells in the anterior portion of MGd were present. This suggests that the cortex posterior and ventral to A1 receives input from anterior MGd.

Thalamocortical connections of R—The rostral auditory area, R, was targeted in two grey squirrels, and in both cases, the injection cores appeared to be completely confined to the architectonically and physiologically defined borders of R (Figs. 7 and 8). Similar patterns of labeled cells were observed in both cases. Dense foci of labeled cells were present in MGv throughout its anterior-posterior length, and some labeled cells were present in the posterior portion of MGm.

The results indicate that the major source of thalamic projections to R is from MGv, and a minor source is from the posterior region of MGm. MGv projects densely to both A1 and R. Comparisons across cases suggests that at least parts of MGv project to both fields, but this would be known with more assurance if separate, distinguishable tracers had been injected in R and A1 of the same case.

Thalamocortical connections of Ti—There are three cases in which Ti was targeted. In case 07-41 (Fig. 9), a CTB injection was confined within the architectonic boundaries of Ti. The CTB injection labeled dense foci of cells in both MGd and SG, with a few cells in the posterior portion of MGm. No labeled cells were present in neither the pulvinar nor the MGv. In the same case, a larger DY injection was centered in Ti, while some of the core included Tm. The anterior portion of MGd had the highest concentration of DY labeled cells. There were also a few DY-labeled cells present in the posterior parts of SG and MGm.

In addition, there were a number of labeled cells in the pulvinar. As pulvinar cells were not labeled by the injection confined to Ti, the labeled pulvinar cells can be attributed to the involvement of Tm in the injection core. A small injection of FR in case 07-41 was centered on the Ti-Tm border. Labeled cells were found in the MGd, SG and MGm, as well as in the pulvinar. In case 07-47 (Fig. 10), a FG injection was in the posterior portion of Ti and spread posteriorly into Tm. FG-labeled cells were present in the pulvinar and MGd. In a third case (07-100, Fig. 11), a small CTB injection confined to the caudal portion of Ti labeled cells in MGd and the anterior portion of MGm.

The results from these injections indicate that MGd is a major source of thalamic projections to the area Ti, with some projections from the posterior portion of MGm. There was no evidence for inputs from MGv. When injections involved both Ti and Tm, labeled neurons were observed in the pulvinar as well, suggesting that the pulvinar projects to Tm. The CTB injection in 07-41 that is more anterior than any of the other injections in Ti, labeled cells in the SG, in addition to MGd and posterior MGm. Thus, anterior Ti appears to receive SG inputs, in addition to those form MGd and MGm, while posterior Ti does not.

Thalamocortical connections of Tp—Four injections in two cases (07-100, Fig. 11, and 07-97, Fig. 12) had injections that were confined to the architectonically defined area Tp. These injections labeled large populations of cells in the pulvinar and MGd, and a few cells in the posterior region of MGm. In both cases, 07-100 (Fig. 11) and 07-91 (Fig. 12), with two injections in Tp, the more anterior injections labeled neurons in a more ventral location in the anterior pulvinar than the more posterior injections. Thus, the anterior pulvinar appears to project in a topographic pattern to Tp. In a third case (07-19, Fig. 13), a DY injection appeared to be on the border of Tp and Tm. DY labeled cells were present in the pulvinar, MGd and the posterior region of MGm. Thus connections were not notably different from those of Tp alone.

In summary, injections in Tp labeled a large concentration of cells in the pulvinar and MGd, and a small concentration of cells in posterior MGm. The labeling pattern was similar when an injection involved both Tp and Tm, suggesting that there is some overlap in thalamocortical projections to these two areas. Evidence presented below suggests that Tm receives pulvinar inputs, but not MGd and MGM inputs.

Thalamocortical connections of Tm—In case 07-47 (Fig. 10), a small FR injection confined to Tm labeled cells in the pulvinar. Another FR injection in case 07-41 (Fig. 9) was in Tm, but spread rostrally into Ti. This injection labeled cells in the pulvinar, MGd and posterior MGm. In other cases where the injections were placed in Ti and spread into Tm, labeled cells were present in the pulvinar in addition to the labeling that resulted from an injection in Ti (e.g. case 07-41, Fig. 9). A DY injection in case 07-49 (Fig. 11) was in both Tm and Tp, and it labeled cells in the pulvinar, MGd and posterior MGm.

In summary, an injection confined in Tm only labeled cells in the pulvinar. Injections that involved both Tm and Ti labeled cells in the pulvinar, MGd and posterior MGm, while injections that involve Ti only label cells in MGd and posterior MGm. As such, it is likely that Tm receives projections mainly, or only from the pulvinar. When the injection involved both Tp and Tm, the labeling pattern was the same as when the injection site only involved Tp. This is suggests that the pulvinar has projections to both Tp and Tm, while MGd and posterior MGm have projections to only Tp and not Tm.

Discussion

In the present study, the thalamic connections of three architectonically distinct subdivisions of temporal cortex in grey squirrels were revealed by injections of retrogradely transported tracers into these subdivisions. Distributions of labeled neurons were related to architectonically identified nuclei of the dorsal thalamus in the same cases, and the cortical injections were localized relative to the boundaries of cortical fields that were apparent in cortical sections parallel to the surface of flattened cortex. The main results are summarized in Fig. 14. Here we relate the results to other relevant findings in squirrels and other rodents, and discuss the implications of the results from sensory processing.

The anterior temporal region, Ta

The Ta regions of temporal cortex in squirrels (Kaas et al., 1972) contains two primary or core auditory fields identified in microelectrode recording experiments as the primary area, A1, and the rostral area, R (Merzenich et al., 1976). Injections of tracers into A1 and R labeled terminations and neurons in other parts of Ta, especially the more dorsal parts of Ta, of both cerebral hemispheres. An injection just ventral to A1 in Ta labeled terminations and neurons in A1 and R, as well as other parts of Ta of both hemispheres (Leuthke et al., 1988). Thus, patterns of cortical connections as well as recording from A1 and R implicate most or all of Ta in auditory processing. The dorsal part of Ta contains the primary areas, A1 and R, while the ventral part of Ta likely includes several secondary auditory fields.

The present results are consistent with the interpretation that Ta is mainly or completely auditory in function. Injections in either A1 or R labeled neurons mainly in the ventral nucleus, MGv, of the medial geniculate complex. A few neurons were also labeled in the medial or magnocellular division, MGm. These observations in squirrels are highly consistent with the reported connections of core auditory fields in other rodents, as well as other mammals in general. While the organization of auditory cortex in rodent species has been variously described, two core fields have been commonly reported, an anterior auditory field, AAF, and a primary auditory area, A1 (e.g. Thomas et al., 1993; Rutkowski et al., 2003; Polley et al., 2007). Descriptions of secondary fields are more varied. The major thalamic inputs to AAF and A1 are from MGv (LeDoux et al., 1985; Roger and Arnault, 1989; Kimura et al., 2003). Two similar fields, AAF and A1 have been described in cats and other carnivores (Knigher, 1977; Reale and Imig, 1980; Merzenich et al., 1973). Both of these fields receive their dominant thalamic inputs from MGv. Likewise, two major core auditory fields, A1 and a rostral area, R, of monkeys, receive inputs from MGv (Morel et al., 1993; Rauschecker, 1997; Kaas et al., 1999; Kaas and Hackett, 2000; de la Mothe et al., 2006;). Additional, but less dense inputs to these core areas in rodents, carnivores, and primates come from MGm, and sometimes MGd. Non-primary auditory areas in these mammals receive most of their auditory inputs from MGm and MGd, and little or none from MGv. Thus, the dense MGv inputs to areas R and A1 in squirrels firmly establishes them as core or primary-like auditory areas. However, their homologies with core areas in other rodents and other mammals remains uncertain, as the reported tonotopic organizations of A1 and R in squirrels (Merzernich et al., 1976) do not correspond with the tonotopic patterns reported for A1 and AAF of other rodents.

The more ventral part of Ta in squirrels remains to be explored in terms of patterns of tonotopic organization, and cortical and subcortical patterns of connections. What is presently clear is that connections with A1 and R exist, and that ventral Ta has a well-developed layer 4 and other histological characteristics of sensory cortex. Thus, we propose that the major secondary auditory fields of squirrels occupy most or all of ventral Ta. Overall, the well-differentiated auditory cortex, as well as the large and distinct auditory nuclei in the thalamus, suggest that audition is an important modality in squirrels.

The medial geniculate complex

As far as we know, the present report provides the first extensive description of the medial geniculate complex in squirrels. The complex as a whole was identified as the medial geniculate, MG, in Nissl and myelin stained brain sections by Kaas et al. (1972), and both MGv and MGd were denoted in Nissl stained sections by Robson and Hall (1977). In the present study, nuclei of the medial geniculate complex were identified in Nissl, myelin, cytochrome oxidase, VGluT2, calbindin (CB), parvalbumin (PV), SMI-32 and AChE preparations (Fig. 3). In Nissl and myelin stained section, medial geniculate nuclei appears to be more distinctly differentiated in squirrels than in rats (Winer et al., 1999; Clerici and Coleman, 1990) or mice (Cruikshank et al., 2001). As with mice (Cruikshank et al., 2001), rabbits (de Venecia et al., 1995; McMullen et al., 1994), as well as monkeys (Molinari et al., 1995; Hackett et al., 1998), the ventral nucleus, MGv, expressed little CB and considerable PV in squirrels, while the dorsal nucleus MGd expressed more CB and little PV. The magnocellular nucleus, MGm, expressed more PV than expected from these other reports, but is similar to the predominance of PV expression in MGv and MGm of monogolian gerbils (Budinger et al., 2000). Nuclei expressing large amounts of PV are those expected to project to primary sensory areas (Jones and Hendry, 1989; Rausell and Jones, 1991; Hashikawa et al., 1991; Diamond et al., 1991). Likewise, thalamic nuclei expressing VGluT2 are those likely to project to core sensory areas of cortex (Fujiyama et al., 2001; Kaneko and Fujiyama, 2002; Nahami and Erisir, 2005; Graziano et al., 2008), and MGv of squirrels expressed more VGluT2 than MGd or MGm. Thalamic nuclei with high levels of metabolic activity are thought to have higher levels of CO (Wong-Riley, 1979), as shown in MGv of squirrels, as well as other mammals (e.g. Hackett et al., 1998). Finally, the denser distribution of the SMI-32 antigen and AChE in MGv than MGd helped characterize nuclei of the MG complex in squirrels (see Jones, 2007 for the distribution of AChE in auditory thalamus of rats).

The temporal intermediate region, Ti

Previous to the present study, we had little understanding of the functional significance of the Ti region. The architectonic characteristics of Ti, including poor myelination, and low cell packing density and weak VGluT2 expression in layer 4, suggested that the area is largely devoted to processing cortical inputs rather than those from primary thalamic sensory nuclei (Fig. 2; also see Wong and Kaas, 2008). By position relative to auditory areas in Ta and visual areas in areas 17, 18, and 19, Ti could be involved in processing visual or auditory information, or both. However, Ti appears to receive little or no visual projections from areas 17 or 18 (Kaas et al., 1989), and only sparse inputs from auditory fields in Ta, which are mainly localized to anterior Ti (Leuthke et al., 1988). The present results, which include those from injections of tracers in the posterior part of Ti, indicate that much of Ti receives inputs from the dorsal nucleus (MGd) of the medial geniculate complex, and the suprageniculate nucleus. Sparse inputs were from MGm. Both MGd and MGm are considered to be auditory nuclei, but neurons within them are more varied in their responses to sounds than in MGv, and they often have longer response latencies and are less sharply selective for tones of specific frequencies (see Jones, 2007 for review). In addition, neurons in MGm may respond to somatosensory stimuli. These nuclei are also thought to project broadly to auditory cortex, including secondary areas with weak or no tonotopic organization. The suprageniculate nucleus (SG), which can be difficult to identify in rodents, is considered to be part of the posterior group of thalamic nuclei (Rockel et al., 1972;Neylon and Haight, 1983;Jones, 2007). SG has inputs from the deeper layers of the superior colliculus and appears to have multisensory functions (Morest, 1965;Oliver and Hall, 1978;Morest and Winer, 1986;Benedek et al., 1996). SG of rats projects to the auditory, insular (Kuypers et al., 1980), and frontal (Kurokawa et al., 1990) cortex, and has been suggested to be responsible for the integration of acoustic and eye movement information

(Kurokawa and Saito, 1995). In cats and monkeys, projections are to higher order areas of the insular region of cortex (e.g. Burton and Jones, 1976;Winer et al., 1977; Mesulum and Mufson, 1985). Thus, the projections of MGd, SG, and MGm implicate the Ti region of squirrels in multisensory, higher-order functions.

In rats, the less densely myelinated region posterior to primary auditory cortex was termed temporal area 2 (Te2) by Zilles and Wree (1985). Te2 was considered part of the auditory belt, rather than the core. In rats, the Te2 region receives afferents from the MGd, MGm, and SG (Arnault and Roger, 1990; Celrici and Coleman, 1990), just as Ti does in squirrels. Thus Ti of squirrels appears to largely correspond to Te2 of rats.

The temporal posterior region, Tp

Most of the cortex just posterior to Ti is within the densely myelinated temporal posterior area we term Tp. The dense myelination of Tp, together with a layer 4 that is densely packed with darkly stained cells (Fig. 2), and other architectonic features (Wong and Kaas, 2008), suggest that Tp is involved in sensory processing, and received sensory inputs from the thalamus. Present results indicate that Tp receives major inputs from the pulvinar nucleus of the visual pulvinar, especially the posterior part that receives dense inputs from the superior colliculus (Robson and Hall, 1977). Other inputs are from MGd, and a minor input to Tp comes from MGm. Previously, Robson and Hall (1977), placed a lesion in the posterior part of the pulvinar complex in a squirrels, and got dense degeneration of axon terminals in Tp and Tm (their 19p). A more anterior lesion of the pulvinar produced dense degeneration in area 19, but very little in Tp. An injection of horseradish peroxidase at the Ti-Tp border labeled neurons in the posterior pulvinar, as expected for the partial involvement of Tp, but also in the dorsal medial geniculate nucleus, MGd. Thus, Tp is strongly implicated in visual processing of a relay of inputs from the extremely large superior colliculus of squirrels (Abplanalp, 1970), via the large and well-differentiated pulvinar. Tp appears to get little or no visual inputs from area 17 and 18 (Kaas et al., 1989), although inputs from the region of area 19 may exist. In ground squirrels, the cortex between area 18 and Tp has been shown to be responsive to visual stimuli (Paolini and Sereno, 1998), and this region receives area 17 and area 18 inputs in grey squirrels (Kaas et al., 1989).

Squirrels retain the capacity to discriminate visual patterns after lesions of all of areas 17 and 18, when areas Tp, Tm, and much of area 19 remain (Wagor, 1978). This remaining visual capacity suggests that the relay of visual information from the superior colliculus, via the pulvinar, to Tp preserves some of the visual functions of temporal cortex in squirrels. As in most mammals, the dorsal lateral geniculate nucleus of squirrels projects almost exclusively to area 17 (Prabhalkor, 1962; Kaas et al., 1972; Robson and Hall, 1977). Rats appear to have no densely myelinated region in temporal cortex posterior to the lightly myelinated area Te2 (Zilles and Wree, 1985). Thus Tp may be a specialization of visual cortex in the highly visual squirrels.

The temporal medial region, Tm

The temporal medial region is not that distinct from Tp in myelin preparations (Fig. 2) and other preparations. As the Tm region was more myelinated and had a darker, dense layer 4 in Nissl preparations, much of the region was distinguished from the adjoining area 19 as “peripheral 19” or “19p” by Kaas et al., (1972). This term was used for the strip of cortex in the lateral border of area 19, with inputs from the posterior pulvinar by Robson and Hall (1977). Our recent, more comprehensive study of the cortical architecture in squirrels further indicated that “19p” and adjoining cortex was very much like Tp in histological appearance, and we renamed “19p” as the temporal medial area, Tm. Due to the similarity in architecture, the exact boundary between Tm and Tp was somewhat uncertain, and the

possibility had remained that they are parts of a single field. Indeed, present results and those of Robson and Hall (1977) indicate that Tm and Tp have similar connections with the posterior pulvinar. However, it also appears from present results that Tm does not have the auditory inputs from MGd and MGm that characterize Tp. Thus, Tm appears to be more solely visual in function, possibly getting some, but not dense, inputs from area 18 (Kaas et al., 1989), as well as from the visual pulvinar.

Conclusions

The thalamic connections of the three major architectonic divisions of temporal cortex in squirrels, regions Ta, Ti and Tp, plus Tm, provide a start in understanding their functional roles. Clearly Ta is highly involved in processing auditory information, Ti, in auditory and multisensory information, and Tp and Tm in visual information. Somewhat surprisingly, Tp also has inputs from the dorsal and medial auditory nuclei, suggesting a role in multisensory processing. Ta is known to contain several auditory fields. Less is known about the Ti, Tm and Tp regions, but these regions may also have subdivisions that mediate similar but slightly different functions.

Acknowledgments

This research was supported by a grant from the National Eye Institute, EY 02686 to J.H.K.

We thank Dr. Troy Hackett for help in identifying the subdivisions of the auditory thalamus in squirrels. Laura Trice provided technical support.

References

Abplanalp P. Some subcortical connections of the visual system in tree shrews and squirrels. Brain Behav Evol. 1970; 3(1):155–168. [PubMed: 5522341]

Arnault P, Roger M. Ventral temporal cortex in the rat: connections of secondary auditory areas Te2 and Te3. J Comp Neurol. 1990; 302(1):110–123. [PubMed: 1707895]

Benedek G, Fischer-Szatmari L, Kovacs G, Perenyi J, Katoh YY. Visual, somatosensory and auditory modality properties along the feline suprageniculate-anterior ectosylvian sulcus/insular pathway. Prog Brain Res. 1996; 112:325–334. [PubMed: 8979839]

Budinger E, Heil P, Scheich H. Functional organization of auditory cortex in the Mongolian gerbil (Meriones unguiculatus). IV. Connections with anatomically characterized subcortical structures. Eur J Neurosci. 2000; 12(7):2452–2474. [PubMed: 10947822]

Burton H, Jones EG. The posterior thalamic region and its cortical projection in New World and Old World monkeys. J Comp Neurol. 1976; 168(2):249–301. [PubMed: 821975]

Campbell MJ, Morrison JH. Monoclonal antibody to neurofilament protein (SMI-32) labels a subpopulation of pyramidal neurons in the human and monkey neocortex. J Comp Neurol. 1989; 282(2):191–205. [PubMed: 2496154]

Celio MR. Parvalbumin in most gamma-aminobutyric acid-containing neurons of the rat cerebral cortex. Science. 1986; 231(4741):995–997. [PubMed: 3945815]

Clerici WJ, Coleman JR. Anatomy of the rat medial geniculate body: I. Cytoarchitecture, myeloarchitecture, and neocortical connectivity. J Comp Neurol. 1990; 297(1):14–31. [PubMed: 2376630]

Condé F, Lund JS, Lewis DA. The hierarchical development of monkey visual cortical regions as revealed by the maturation of parvalbumin-immunoreactive neurons. Brain Res Dev Brain Res. 1996; 96(1–2):261–276.

Cruikshank SJ, Killackey HP, Metherate R. Parvalbumin and calbindin are differentially distributed within primary and secondary subregions of the mouse auditory forebrain. Neuroscience. 2001; 105(3):553–569. [PubMed: 11516823]

de la Mothe LA, Blumell S, Kajikawa Y, Hackett TA. Thalamic connections of the auditory cortex in marmoset monkeys: core and medial belt regions. J Comp Neurol. 2006; 496(1):72–96. [PubMed: 16528728]

de Venecia RK, Smelser CB, Lossman SD, McMullen NT. Complementary expression of parvalbumin and calbindin D-28k delineates subdivisions of the rabbit medial geniculate body. J Comp Neurol. 1995; 359(4):595–612. [PubMed: 7499550]

DeFelipe J. Types of neurons, synaptic connections and chemical characteristics of cells immunoreactive for calbindin-D28K, parvalbumin and calretinin in the neocortex. J Chem Neuroanat. 1997; 14:1–19. [PubMed: 9498163]

Diamond IT, Fitzpatrick D, Schmechel D. Calcium-binding proteins distinguish large and small cells of the ventral posterior and lateral geniculate nuclei of the prosimian galago and tree shrew (Tupaia belangeri). Proc Natl Acad Sci U S A. 1993; 90(4):1425–1429. [PubMed: 8434002]

Fujiyama F, Furuta T, Kaneko T. Immunocytochemical localization of candidates for vesicular glutamate transporters in the rat cerebral cortex. J Comp Neurol. 2001; 435(3):379–387. [PubMed: 11406819]

Gallyas F. Silver staining of myelin by means of physical development. Neurol Res. 1979; 1(2):203–209. [PubMed: 95356]

Graziano A, Liu XB, Murray KD, Jones EG. Vesicular glutamate transporters define two sets of glutamatergic afferents to the somatosensory thalamus and two thalamocortical projections in the mouse. J Comp Neurol. 2008; 507(2):1258–1276. [PubMed: 18181146]

Hackett TA, Stepniewska I, Kaas JH. Thalamocortical connections of the parabelt auditory cortex in macaque monkeys. J Comp Neurol. 1998; 400(2):271–286. [PubMed: 9766404]

Hashikawa T, Rausell E, Molinari M, Jones EG. Parvalbumin- and calbindin-containing neurons in the monkey medial geniculate complex: differential distribution and cortical layer specific projections. Brain Res. 1991; 544(2):335–341. [PubMed: 2039948]

Hof PR, Glezer II, Conde F, Flagg RA, Rubin MB, Nimchinsky EA, Vogt Weisenhorn DM. Cellular distribution of the calcium-binding proteins parvalbumin, calbindin, and calretinin in the neocortex of mammals: phylogenetic and developmental patterns. J Chem Neuroanat. 1999; 16(2):77–116. [PubMed: 10223310]

Ichinohe N, Fujiyama F, Kaneko T, Rockland KS. Honeycomb-like mosaic at the border of layers 1 and 2 in the cerebral cortex. J Neurosci. 2003; 23(4):1372–1382. [PubMed: 12598625]

Jones, EG. Thalamus: Cambridge University Press; 2007.

Jones EG, Hendry SH. Differential calcium binding protein immunoreactivity distinguishes classes of relay neurons in monkey thalamic nuclei. Eur J Neurosci. 1989; 1(3):222–246. [PubMed: 12106154]

Kaas JH, Hackett TA. Subdivisions of auditory cortex and processing streams in primates. Proc Natl Acad Sci U S A. 2000; 97(22):11793–11799. [PubMed: 11050211]

Kaas JH, Hackett TA, Tramo MJ. Auditory processing in primate cerebral cortex. Curr Opin Neurobiol. 1999; 9(2):164–170. [PubMed: 10322185]

Kaas JH, Hall WC, Diamond IT. Visual cortex of the grey squirrel (Sciurus carolinensis): architectonic subdivisions and connections from the visual thalamus. J Comp Neurol. 1972; 145(3):273–305. [PubMed: 5030907]

Kaas JH, Krubitzer LA, Johanson KL. Cortical connections of areas 17 (V-I) and 18 (V-II) of squirrels. J Comp Neurol. 1989; 281(3):426–446. [PubMed: 2703555]

Kaneko T, Fujiyama F. Complementary distribution of vesicular glutamate transporters in the central nervous system. Neurosci Res. 2002; 42(4):243–250. [PubMed: 11985876]

Kimura A, Donishi T, Sakoda T, Hazama M, Tamai Y. Auditory thalamic nuclei projections to the temporal cortex in the rat. Neuroscience. 2003; 117(4):1003–1016. [PubMed: 12654352]

Knight PL. Representation of the cochlea within the anterior auditory field (AAF) of the cat. Brain Res. 1977; 130:447–467. [PubMed: 890444]

Krubitzer LA, Kaas JH. Thalamic connections of three representations of the body surface in somatosensory cortex of gray squirrels. J Comp Neurol. 1987; 265(4):549–580. [PubMed: 2448348]

Kurokawa T, Saito H. Retrograde axonal transport of different fluorescent tracers from the neocortex to the suprageniculate nucleus in the rat. Hear Res. 1995; 85(1–2):103–108. [PubMed: 7559164]

Kurokawa T, Yoshida K, Yamamoto T, Oka H. Frontal cortical projections from the suprageniculate nucleus in the rat, as demonstrated with the PHA-L method. Neurosci Lett. 1990; 120(2):259–262. [PubMed: 1705683]

Kuypers HG, Bentivoglio M, Catsman-Berrevoets CE, Bharos AT. Double retrograde neuronal labeling through divergent axon collaterals, using two fluorescent tracers with the same excitation wavelength which label different features of the cell. Exp Brain Res. 1980; 40(4):383–392. [PubMed: 6160043]

LeDoux JE, Ruggiero DA, Reis DJ. Projections to the subcortical forebrain from anatomically defined regions of the medial geniculate body in the rat. J Comp Neurol. 1985; 242(2):182–213. [PubMed: 4086664]

Luethke LE, Krubitzer LA, Kaas JH. Cortical connections of electrophysiologically and architectonically defined subdivisions of auditory cortex in squirrels. J Comp Neurol. 1988; 268(2):181–203. [PubMed: 3360984]

McMullen NT, Smelser CB, de Venecia RK. A quantitative analysis of parvalbumin neurons in rabbit auditory neocortex. J Comp Neurol. 1994; 349(4):493–511. [PubMed: 7860786]

Merzenich MM, Kaas JH, Roth GL. Auditory cortex in the grey squirrel: tonotopic organization and architectonic fields. J Comp Neurol. 1976; 166(4):387–401. [PubMed: 1270613]

Merzenich MM, Knight PL, Roth GL. Cochleotopic organization of primary auditory cortex in the cat. Brain Res. 1973; 63:343–346. [PubMed: 4764302]

Mesulam M, Mufson EJ. Insular of Reil in man and monkeys. Cereb Cortex. 1985; 4:179–225.

Mesulam MM. Tetramethyl benzidine for horseradish peroxidase neurohistochemistry: a non-carcinogenic blue reaction product with superior sensitivity for visualizing neural afferents and efferents. J Histochem Cytochem. 1978; 26(2):106–117. [PubMed: 24068]

Molinari M, Dell'anna ME, Rausell E, Leggio MG, Hashikawa T, Jones EG. Auditory thalamocortical pathways defined in monkeys by calcium-binding protein immunoreactivity. J Comp Neurol. 1995; 362(2):171–194. [PubMed: 8576432]

Morel A, Garraghty PE, Kaas JH. Tonotopic organization, architectonic fields, and connections of auditory cortex in macaque monkeys. J Comp Neurol. 1993; 335(3):437–459. [PubMed: 7693772]

Morest DG. The lateral tegmental system of the midbrain and the medial geniculate body: study with Golgi and Nauta methods in cat. J Anat. 1965; 99:611–634. [PubMed: 17105147]

Morest DK, Winer JA. The comparative anatomy of neurons: homologous neurons in the medial geniculate body of the opossum and the cat. Adv Anat Embryol Cell Biol. 1986; 97:1–94. [PubMed: 3529846]

Nahmani M, Erisir A. VGluT2 immunochemistry identifies thalamocortical terminals in layer 4 of adult and developing visual cortex. J Comp Neurol. 2005; 484(4):458–473. [PubMed: 15770654]

Neylon L, Haight JR. Neocortical projections of the suprageniculate and posterior thalamic nuclei in the marsupial brush-tailed possum, Trichosurus vulpecula (Phalangeridae), with a comparative commentary on the organization of the posterior thalamus in marsupial and placental mammals. J Comp Neurol. 1983; 217(4):357–375. [PubMed: 6886058]

Oliver DL, Hall WC. The medial geniculate body of the tree shrew, Tupaia glis. I. Cytoarchitecture and midbrain connections. J Comp Neurol. 1978; 182(3):423–458. [PubMed: 102660]

Paolini M, Sereno MI. Direction selectivity in the middle lateral and lateral (ML and L) visual areas in the California ground squirrel. Cereb Cortex. 1998; 8(4):362–371. [PubMed: 9651131]

Polley DB, Read HL, Storace DA, Merzenich MM. Multiparametric auditory receptive field organization across five cortical fields in the albino rat. J Neurophysiol. 2007; 97(5):3621–3638. [PubMed: 17376842]

Prabhakar VG. Visual radiations in mammals with pure-cone retinae. J Comp Neurol. 1962; 119(2): 201–210. [PubMed: 13995742]

Rausell E, Jones EG. Chemically distinct compartments of the thalamic VPM nucleus in monkeys relay principal and spinal trigeminal pathways to different layers of the somatosensory cortex. J Neurosci. 1991; 11(1):226–237. [PubMed: 1702464]

Reale RA, Imig TJ. Tonotopic organization in auditory cortex of the cat. J Comp Neurol. 1980; 192(2): 265–291. [PubMed: 7400399]

Robson JA, Hall WC. The organization of the pulvinar in the grey squirrel (Sciurus carolinensis). II. Synaptic organization and comparisons with the dorsal lateral geniculate nucleus. J Comp Neurol. 1977; 173(2):389–416. [PubMed: 853144]

Rockel AJ, Heath CJ, Jones EG. Afferent connections to the diencephalon in the marsupial phalanger and question of sensory convergence in the “posterior group” of the thalamus. J Comp Neurol. 1972; 145(1):105–129. [PubMed: 5036665]

Roger M, Arnault P. Anatomical study of the connections of the primary auditory area in the rat. J Comp Neurol. 1989; 287(3):339–356. [PubMed: 2778109]

Rutkowski RG, Miasnikov AA, Weinberger NM. Characterisation of multiple physiological fields within the anatomical core of rat auditory cortex. Hear Res. 2003; 181(1–2):116–130. [PubMed: 12855370]

Thomas H, Tillein J, Heil P, Scheich H. Functional organization of auditory cortex in the mongolian gerbil (Meriones unguiculatus). I. Electrophysiological mapping of frequency representation and distinction of fields. Eur J Neurosci. 1993; 5(7):882–897. [PubMed: 8281300]

Van Brederode JF, Mulligan KA, Hendrickson AE. Calcium-binding proteins as markers for subpopulations of GABAergic neurons in monkey striate cortex. J Comp Neurol. 1990; 298(1):1–22. [PubMed: 2170466]

Van De Werd HJ, Uylings HB. The rat orbital and agranulat insular prefrontal cortical areas: a cytoarchitectonic and chemoarchitectonic study. Brain Struct Funct. 2008; 212(5):387–401. [PubMed: 18183420]

Wagor E. Pattern vision in the grey squirrel after visual cortex ablation. Behav Biol. 1978; 22(1):1–22. [PubMed: 623604]

Winer JA, Diamond IT, Raczkowski D. Subdivisions of the auditory cortex of the cat: the retrograde transport of horseradish peroxidase to the medial geniculate body and posterior thalamic nuclei. J Comp Neurol. 1977; 176(3):387–417. [PubMed: 915045]

Winer JA, Kelly JB, Larue DT. Neural architecture of the rat medial geniculate body. Hear Res. 1999; 130(1–2):19–41. [PubMed: 10320097]

Wong-Riley M. Changes in the visual system of monocularly sutured or enucleated cats demonstrable with cytochrome oxidase histochemistry. Brain Res. 1979; 171(1):11–28. [PubMed: 223730]

Zilles, K.; Wree, A. Cortex: Areal and laminar structure. GP, editor. Sydney: Academic Press; 1985. p. 375-415.

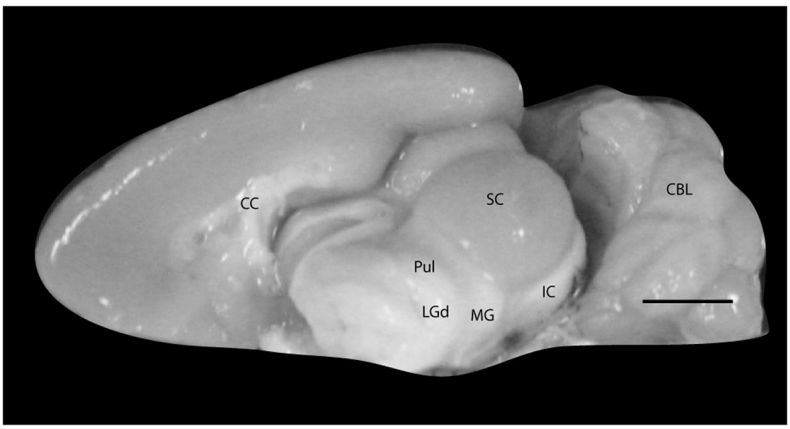

Figure 1.
Medial view of the brain of grey squirrels with the left hemisphere removed to reveal the subcortical structures. Scale bar = 5mm.

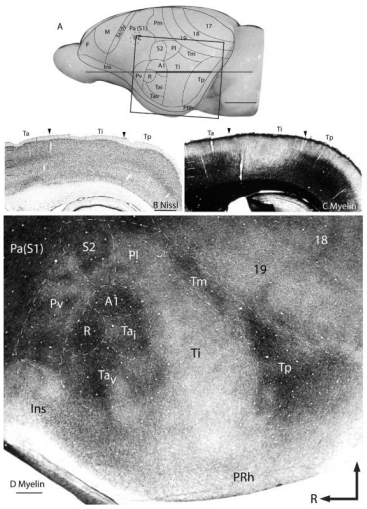

Figure 2.

Architectonic features of the temporal cortex. (A) Representative cortical map superimposed on the lateral view of a grey squirrel brain. The thick part of the horizontal line across the brain indicates the location of the horizontal brain sections illustrated in (B) and (C). (B) Nissl stained horizontal section and (C) adjacent horizontal section stained for myelin. The boxed region in A is shows the location of the artificially flattened brain section processed for myelin shown in (D). Scale bar in (A) = 5mm, for (B), (C), and (D) = 1mm.

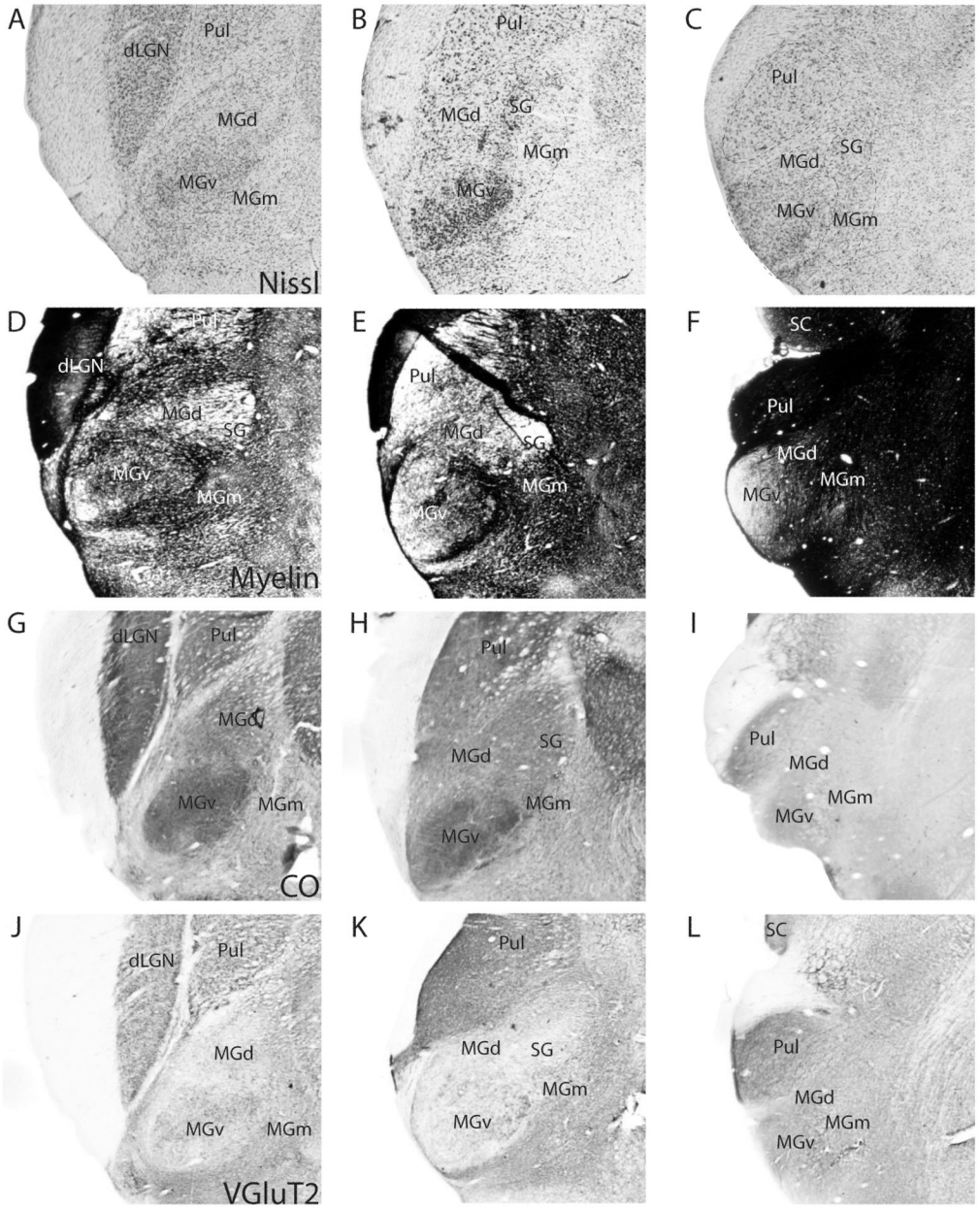

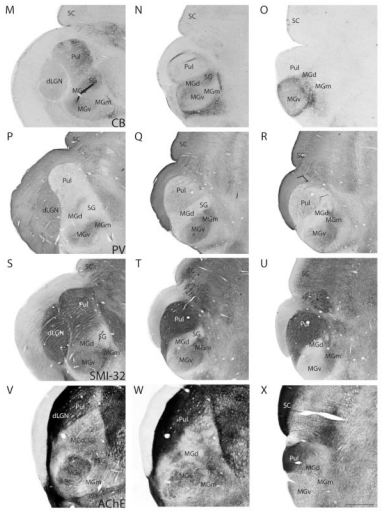

Figure 3.

Architectonic features of thalamic nuclei. Each row contains photomicrographs of sections taken at three representative levels of the thalamus in an anterior to posterior progression. Sections are from two different grey squirrel brains. Scale bar for the sections = 1mm, and is shown in (X).

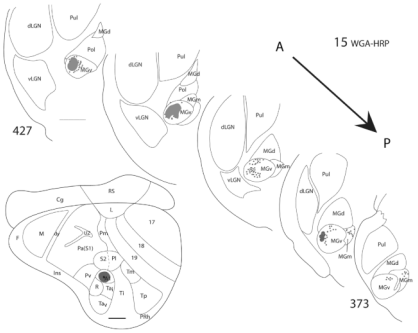

Figure 4.

Thalamic connections of A1 in squirrel 15. The WGA-HRP injection was guided by microelectrode mapping. The injection site is indicated on a representative drawing of the grey squirrel flattened cortex and appears to have been confined to A1. Thalamic sections are arranged in an anterior (section 427) to posterior (section 373) progression. Dots represent the locations of retrogradely labeled cell bodies whereas patches represent the locations of possible anterograde label. Labeled cells are primarily concentrated in MGv. Scale bar for brain = 2mm, for thalamus sections = 1mm.

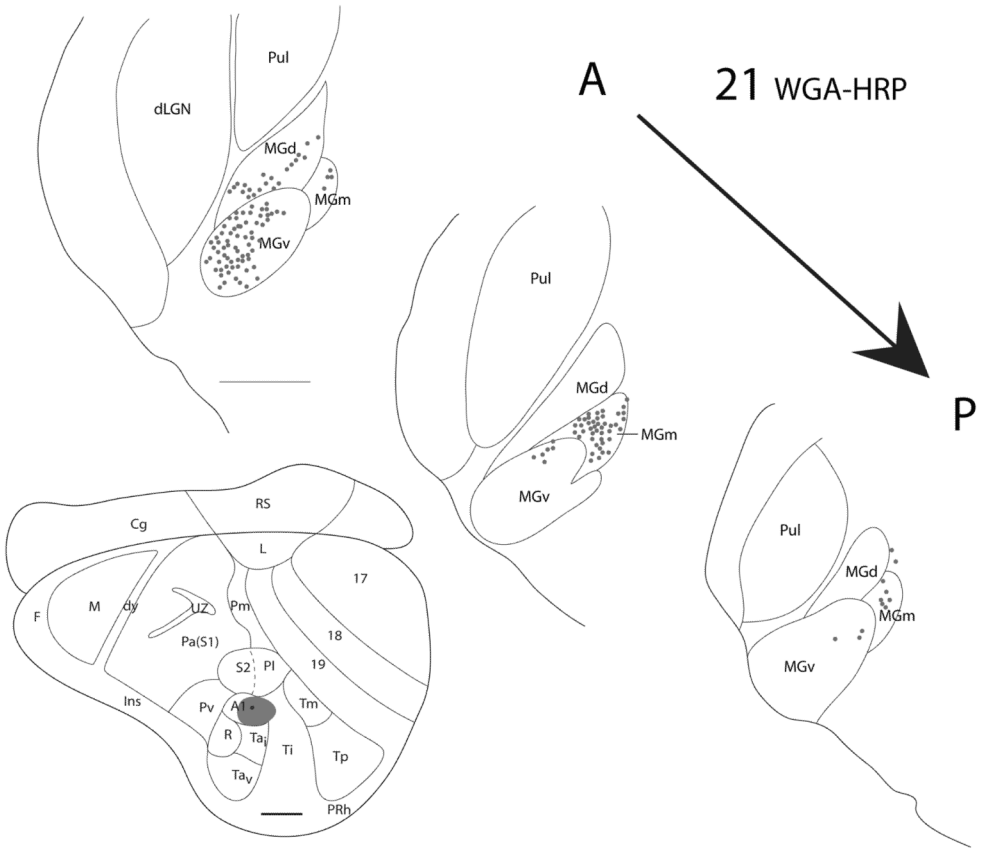

Figure 5.

Thalamic connections of A1 in squirrel 21. The WGA-HRP injection was guided by microelectrode mapping. The injection was mostly within A1 but spread slightly into the cortex caudal to A1. The injection site is indicated on a representative drawing of the grey squirrel flattened cortex. Dots indicate the location of retrogradely labeled cell bodies, and the thalamic sections are arranged in an anterior to posterior progression. Labeled cells are present in MGv, MGd, and MGm. Scale bar for brain = 2mm, for thalamic sections = 1mm.

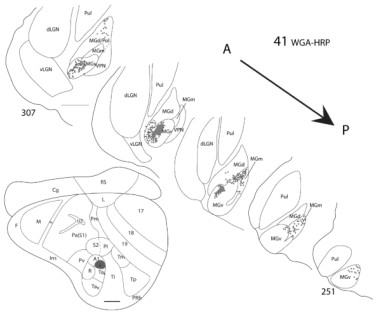

Figure 6.

Thalamic connections of A1 in squirrel 41. The WGA-HRP injection was guided by microelectrode mapping. The injection was mostly within A1 but extended slightly into the cortex ventral to A1 (Tai). The location of the injection site is indicated on a representative drawing of the grey squirrel flattened cortex. Thalamic sections are arranged in an anterior (section 307) to posterior (section 251) progression. Dots indicate the locations of retrogradely labeled cell bodies whereas patches represent the locations of possible anterograde label. Labeled cells are primarily concentrated in MGv and also present in MGm and MGd. Scale bar for brain = 2mm, for thalamic sections = 1mm.

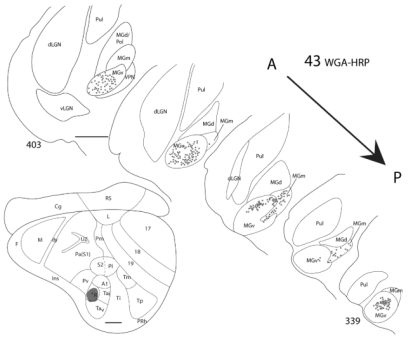

Figure 7.

Thalamic connections of R in squirrel 43. The WGA-HRP injection was guided by micorelectrode mapping. The injection was mostly confined to R, as indicated on the representative drawing of the grey squirrel flattened cortex. Thalamic sections are arranged in an anterior (section 403) to posterior (section 339) progression. Dots indicate the location of retrogradely labeled cell bodies. Labeled cells are primarily concentrated in MGv, but also present in MGm. Scale bar for brain = 2mm, for thalamus sections = 1mm.

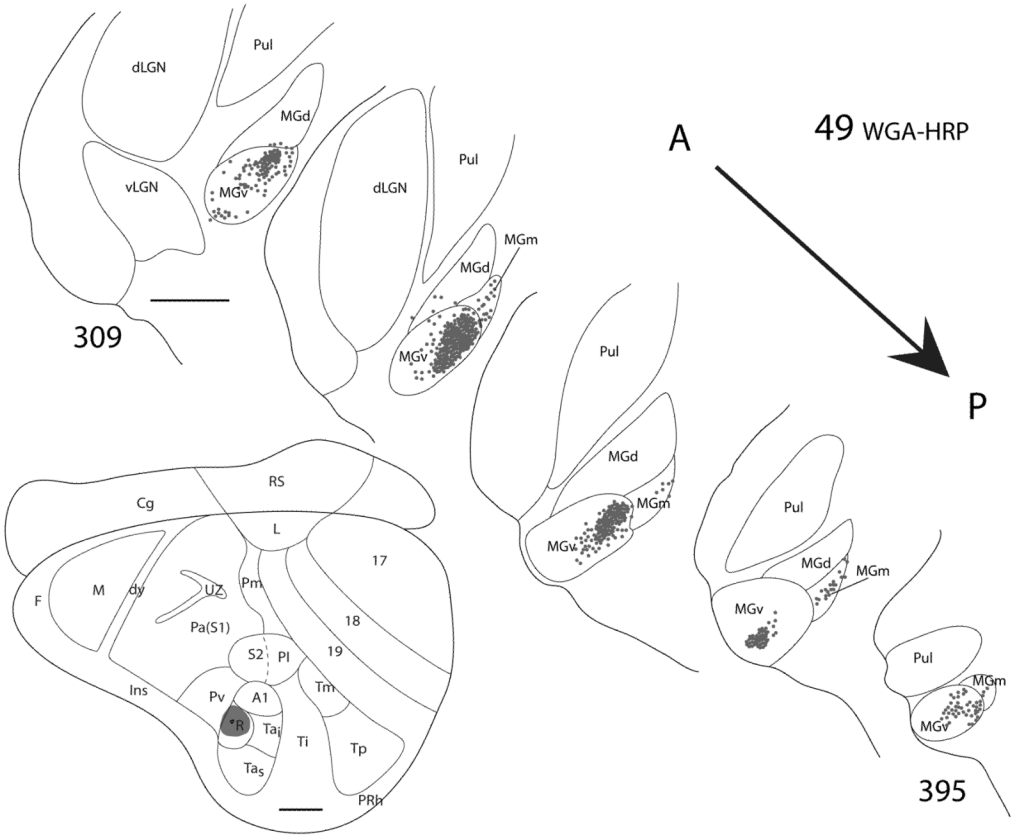

Figure 8.

Thalamic connections of R in squirrel 49. The WGA-HRP injection was guided by micorelectrode mapping. As indicated on the representative drawing of the grey squirrel flattened cortex, the WGA-HRP injection was confined to R. Thalamic sections are arranged in an anterior (section 209) to posterior (section 395) progression. Dots indicate the location of retrogradely labeled cell bodies. Labeled cells are primarily concentrated in MGv, but also present in MGm. Scale bar for brain = 2mm, for thalamus sections = 1mm.

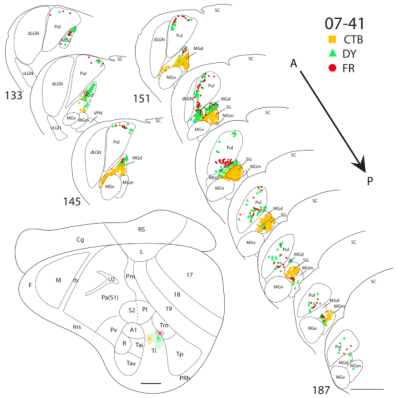

Figure 9.

Thalamic connections of Ti and Tm in squirrel 07-41. Locations of the three different tracer injections, CTB, DY and FR, are indicated on the representative drawing of the grey squirrel flattened cortex. Symbols representing each injection site and their respective retrogradely labeled cells are indicated on the top right corner of the figure. The CTB injection (square) was confined to Ti, whereas the DY (filled triangle) and FR (dot) injections involved both Ti and Tm. Thalamic sections are arranged in an anterior (section 133) to posterior (section 187) progression. CTB labeled cells are primarily concentrated in MGC, whereas FR labeled cells are largely concentrated in pulvinar. DY labeled cells were present in both MGC and pulvinar. Scale bar for brain = 2mm, for thalamic sections = 1mm.

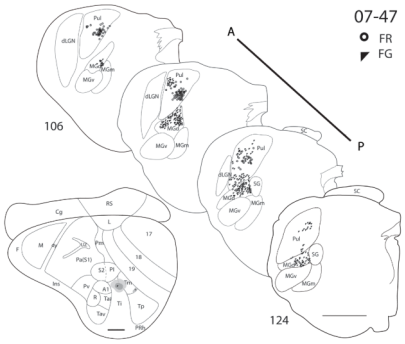

Figure 10.

Thalamic connections of Ti and Tm in squirrel 07-47. Locations of the FR and FG tracer injections are indicated on the representative drawing of the grey squirrel flattened cortex. The FG (filled triangle) injection involved both Ti and Tm, whereas the FR injection (dot) was confined to Tm. Thalamic sections are arranged in an anterior (section 106) to posterior (section 124) progression. FR labeled cells are primarily concentrated in pulvinar, whereas FG labeled cells are present in both pulvinar and MGd. Scale bar for brain = 2mm, for thalamus sections = 1mm.

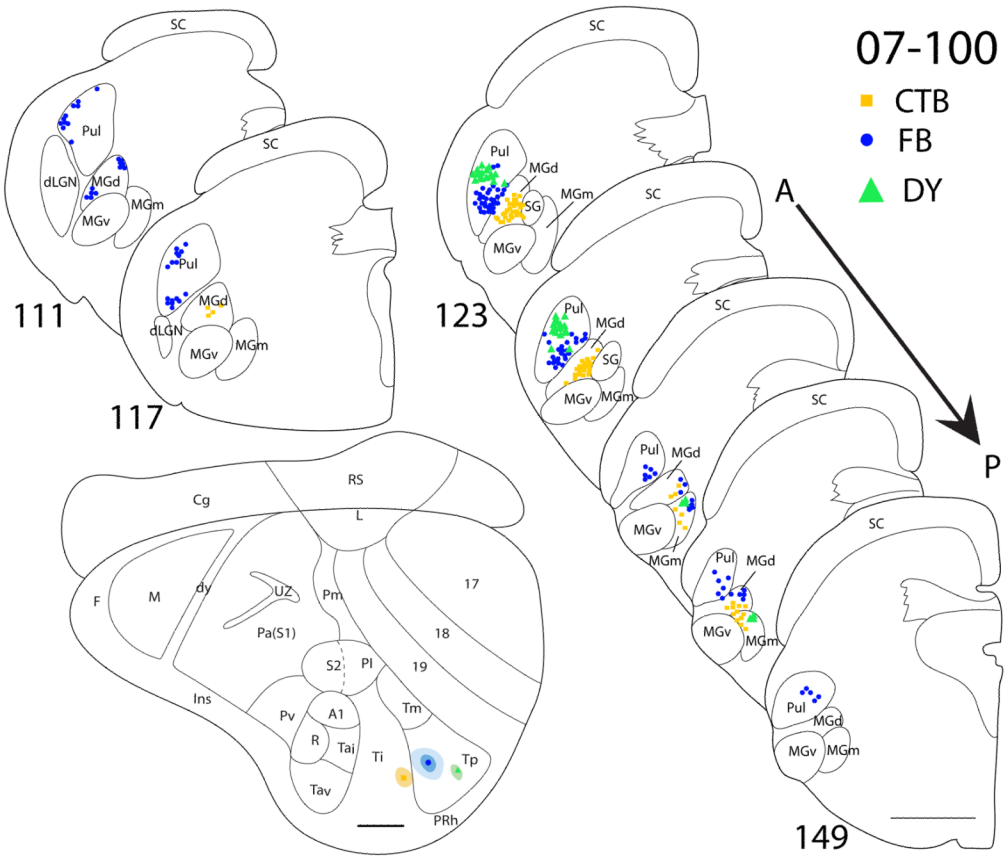

Figure 11.

Thalamic connections of Ti and Tp in squirrel 07-100. Locations of the CTB (square), FB (dot) and DY (filled triangle) injection sites are indicated on the representative drawing of the grey squirrel flattened cortex. The CTB injection was confined to Ti, and the FB and DY injections were confined to Tp. The location of retrogradely labeled CTB, FB and DY cell bodies is indicated on the thalamus sections that are arranged in an anterior (section 111) to posterior (section 149) progression. CTB labeled cells are primarily concentrated in MGm and MGd, whereas DY cells are more prevalent in pulvinar. FB labeled cells are present in pulvinar, MGm and MGd. Scale bar for brain = 2mm, for thalamus sections = 1mm.

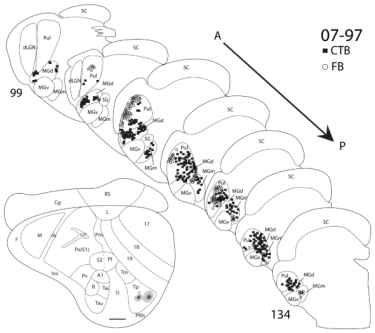

Figure 12.

Thalamic connections of Tp in squirrel 07-97. Both the CTB (filled square) and FB (open circle) injections were confined to Tp, as indicated on the representative drawing of the grey squirrel flattened cortex. The thalamic sections are arranged in an anterior (section 99) to posterior (section 134) progression. Both injections labeled pulvinar as well as MGm and MGd. Scale bar for brain = 2mm, for thalamus sections = 1mm.

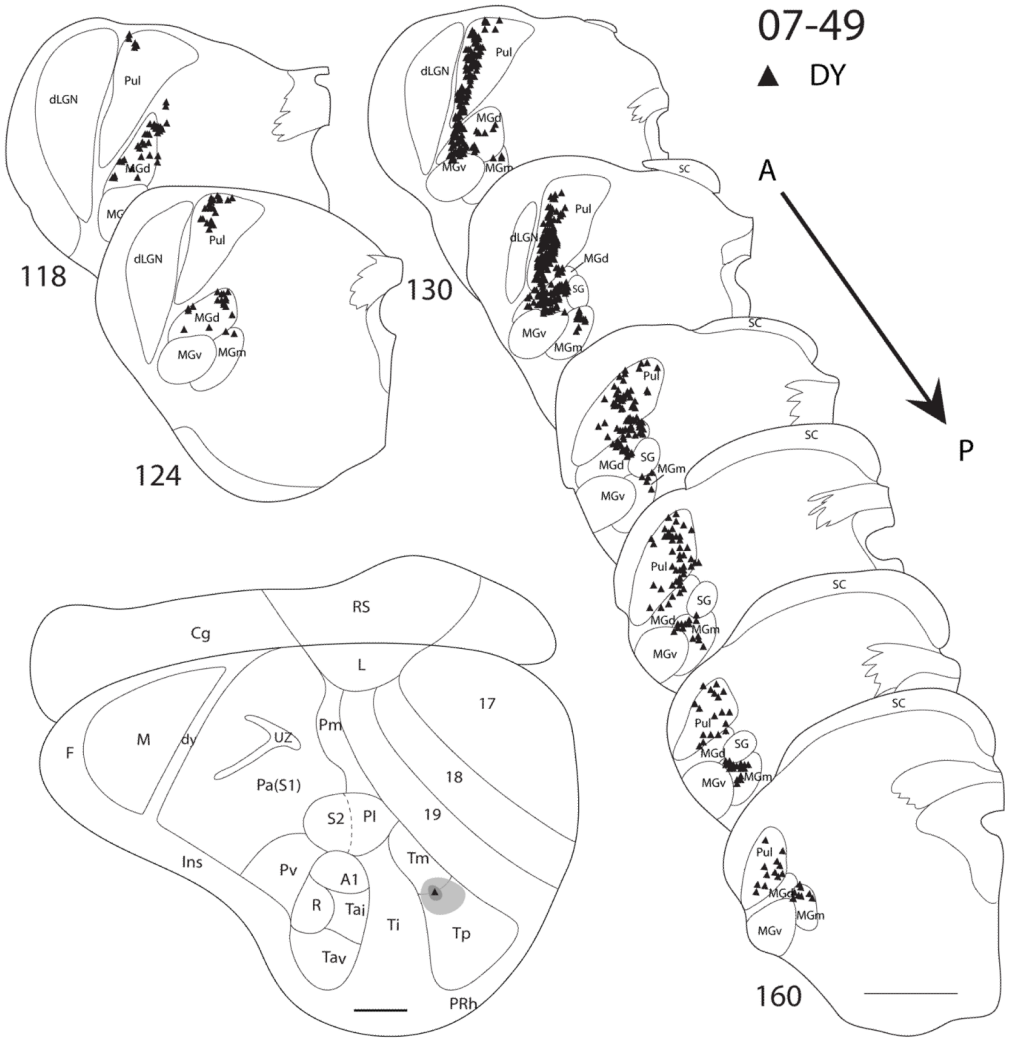

Figure 13.

Thalamic connections of Tm and Tp in squirrel 07-49. The DY injection (filled triangle) is on the border between Tm and Tp as indicated on the representative drawing of the grey squirrel flattened cortex. Thalamic sections are arranged in an anterior (section 118) to posterior (section 160) progression. DY labeled cells are present in pulvinar, MGm, and MGd. Scale bar for brain = 2mm, for thalamus sections = 1mm.

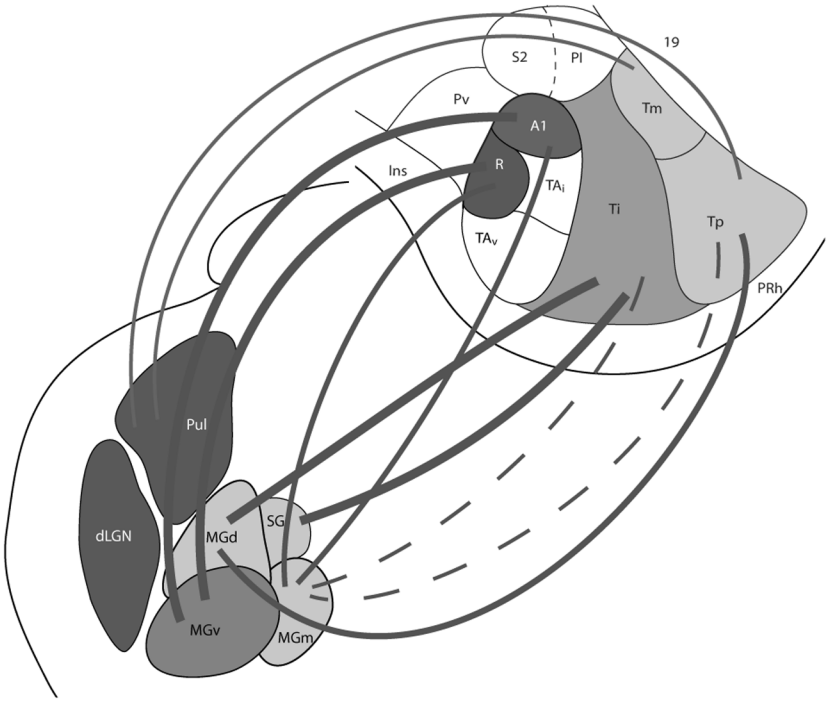

Figure 14.
Summary of the projection patterns of the pulvinar, MGv, MGd, MGm and SG nuclei to temporal cortex in grey squirrels. The thick lines indicate the major source thalamic projections, the thin lines represent weaker projections, and the dotted lines denote sparse projections.

Table 1

List of Abbreviations

3a/dy	Dysgranular area
17	Area 17
18	Area 18
19	Area 19
AChE	Acetylcholine Esterase
CB	Calbindin
CBL	Cerebellum
Cg	Cingulate area
cc	Corpus callosum
CO	Cytochrome oxidase
dLGN	Dorsal lateral geniculate nucleus
dy	Dysgranular region
F	Frontal area
IC	Inferior colliculus
Ins	Insular
L	Limbic
MG	Medial geniculate
MGC	Medial geniculate complex
MGd	Medial geniculate dorsal nucleus
MGm	Medial geniculate magnocellular nucleus
MGv	Medial geniculate ventral nucleus
Pa	Parietal anterior area
Pl	Parietal lateral area
Pm	Parietal medial area
Pol	Posterior lateral nucleus
Pv	Parietal ventral area
PV	Parvalbumin
PRh	Perirhinal area
PB	Phosphate buffer
A1	Primary auditory cortex
M	Primary motor cortex
S1	Primary somatosensory cortex
Pul	Pulvinar
R	Rostral auditory area
RS	Retrosplenial area
S2	Secondary somatosensory cortex
SC	Superior colliculus
SG	Supragenicular
Ta	Temporal anterior area
Ta_i	Temporal anterior intermediate area

Tav	Temporal anterior ventral area
Ti	Temporal intermediate area
Tm	Temporal mediodorsal area
Tp	Temporal posterior area
UZ	Unresponsive zone
VGluT2	Vesicle glutamate transporter 2
vLGN	Ventral lateral geniculate nucleus
VPN	Ventral posterior nucleus

Table 2

Summary of tracers injected in temporal cortex of ten grey squirrels. Injections primary auditory areas were guided by microelectrode mapping. Injection site core is noted in regular font, its diffusion spread into adjoining cortex is indicated by small font.

Case	A1	R	Remainder of TA	Ti	Tm	Tp
15	WGA-HRP					
21	WGA-HRP			WGA-HRP		
41	WGA-HRP		WGA-HRP			
43		WGA-HRP				
49		WGA-HRP				
07-41				CTB/DY/FR	FR/DY	
07-47				FG	FR/FG	
07-49					DY	
07-97						CTB/FB
07-100				CTB		FB/DY

Table 3

Antibody characterization

Antibody	Host (Type)	Source	Catalog #	Dilution factor	Antigen
SMI-32	Mouse (monoclonal)	Covance Inc., Princeton, NJ	SMI-32R	1:2000	Neurofilament H
PV	Mouse (monoclonal)	Sigma-Aldrich, St. Louis, Mo	P3088	1:2000	Frog muscle parvalbumin (Clone PARV-19)
CB	Mouse (monoclonal)	Swant, Bellinzona, Switzerland	C98-48	1:5000	Hybridized mouse myeloma cells with spleen cells from CB D-28k immunized mice
VGluT2	Mouse (monoclonal)	Chemicon now part of Millipore, Billerica, MA	MAB5504	1:2000	Recombinant protein from rat VGluT2